Available online at www.sciencedirect.com
ScienceDirect
Catalysis Today 122 (2007) 341–351
CATALYSIS TODAY
www.elsevier.com/locate/cattod

A comparative study on the selective hydrogenation of α,β unsaturated aldehyde and ketone to unsaturated alcohols on Au supported catalysts

C. Milone [a,*], C. Crisafulli [b], R. Ingoglia [a], L. Schipilliti [a], S. Galvagno [a]

[a] *University of Messina, Department of Industrial Chemistry and Materials Engineering, Faculty of Engineering, Contrada di Dio, I-98166 Messina, Italy*
[b] *University of Catania, Department of Chemistry, Viale A. Doria 5, I-95100 Catania, Italy*

Available online 17 January 2007

Abstract

The hydrogenation of *trans*,4-phenyl,3-buten,2-one (benzalacetone) and *trans*,3-phenyl, propenal (cinnamaldehyde) was carried out on Au supported on iron oxides catalysts. Commercial goethite (FeOOH), maghemite (γFe_2O_3) and hematite (αFe_2O_3) were used as supports. The catalytic activity of Au/Fe_2O_3 reference catalyst, supplied by the World Gold Council, was also investigated. Gold catalysts and the parent supports were characterized by BET, X-ray diffraction (XRD), temperature programmed reduction (TPR), temperature programmed desorption of ammonia (NH_3-TPD) and high resolution transmission electron microscopy (HRTEM).

Among the catalysts investigated Au supported on FeOOH shows the highest activity and selectivity to UA in the hydrogenation of unsaturated carbonyl compounds whereas Au supported on αFe_2O_3 are the less active and selective catalysts.

The catalytic activity and selectivity to unsaturated alcohols (UA) in the hydrogenation of benzalacetone and cinnamaldehyde are less influenced by the morphology of gold particles and are mainly influenced by the nature of the support.

A correlation between the reducibility of the catalysts and the activity and selectivity to UA has been found. Increasing the reducibility of the catalysts both the activity and selectivity to UA increase. These results let us to argue that active and selective sites are formed by negative gold particles formed through the electron transfer from the reduced support to the metal.

Keywords: Gold catalysts; Selective hydrogenation; α,β unsaturated ketone and aldehyde; α,β unsaturated alcohols; Iron oxides

1. Introduction

Gold supported catalysts show a remarkable selectivity towards the hydrogenation of the conjugated C=O bond in the hydrogenation of α,β unsaturated aldehydes [1–5] and ketones [6–8].

The catalytic behavior of gold in the hydrogenation of α,β unsaturated ketones is of a great relevance due to the fact that on classical hydrogenation metal catalysts (Pt, Ru, etc.) the main reaction product is always the saturated ketone [9–11]. The formation of the secondary allylic alcohol is easily achieved under hydrogen transfer conditions [12,13].

Previous studies have demonstrated that in the hydrogenation of benzalacetone on Au supported on iron oxy-hydroxides the selectivity towards the formation of α,β unsaturated alcohol is less influenced by the preparation method, deposition precipitation or coprecipitation [7] whereas it is strongly influenced by the nature of the support [7,8]. The most selective catalysts were obtained when gold was dispersed on goethite (FeOOH), maghemite (γFe_2O_3) and iron oxy-hydroxides prepared by precipitation from a solution of iron nitrate [8]. Au supported on hematite (αFe_2O_3) and Al_2O_3 showed the lowest selectivity [7,8].

From these studies no correlation was drawn between activity and selectivity to unsaturated alcohol (UA) and the morphology of gold particles.

It is known that the role of metal particle size and particle shape is crucial in the catalysis by gold therefore it deserves to be deeply investigated.

The influence of the morphology of gold particles on the catalytic activity has been mainly investigated in the hydrogenation of α,β unsaturated aldehydes and literature data are different and somewhat controversial.

Zanella et al. [5] have reported that the rate of hydrogenation of the C=O group of the crotonaldehyde on Au/TiO_2 is almost

* Corresponding author. Tel.: +39 090 3977242; fax: +39 090 3977464.
E-mail address: cmilone@ingegneria.unime.it (C. Milone).

0920-5861/$ – see front matter
doi:10.1016/j.cattod.2007.01.011

independent from gold particle size when it varies in the range 1.7–8.7 nm.

Hutchings et al. [3] have proposed that active and selective sites for the hydrogenation of but-2-enal on Au/ZnO catalysts are associated with the presence of large Au particles.

Claus et al. [2,14] have reported that in the hydrogenation of acrolein on Au/TiO_2 and Au/ZrO_2 the catalytic activity and selectivity to crotyl alcohol increases with gold particle size.

In a later paper, Claus et al. [15] have identified the edge of gold nanoparticles as active sites in the hydrogenation of acrolein on Au/ZnO catalyst.

The same authors [14] have demonstrated that the particle size dependence of activity and selectivity of gold catalysts in the hydrogenation of acrolein is a cooperative effect of particle size and gold morphology such as degree of rounding and portion of multiple twinned gold particles (MTPs). Gold catalysts having a larger portion of metal particle with a spherical shape, i.e. high degree of rounding, showed the highest catalytic activity and selectivity to allylalcohol [14]. The predominance, instead, of MTPs led to a decrease of TOF and allyl alcohol selectivity.

With respect to the degree of rounding of gold particles it was found that it is influenced by the nature of the support. Claus et al. [16] have reported that on SiO_2 and TiO_2 gold particles are nearly spherical whereas on ZrO_2, ZnO extended facets of gold surface are present.

The aim of this work is to investigate the influence of gold morphology of Au supported on iron oxides in the activity and selectivity to UA in the hydrogenation of α,β unsaturated carbonyl compounds. The reactions investigated are the hydrogenation of *trans*,4-phenyl,3-buten-2-one, (benzalacetone), and *trans*,3-phenyl, propenal (cinnamaldehyde).

Gold catalysts supported on single phase iron oxides such as goethite (FeOOH), maghemite (γFe_2O_3), hematite (αFe_2O_3) have been used together with Au/Fe_2O_3 reference catalyst supplied by the World Gold Council.

A detailed characterization by HRTEM, surface acidity measurements (NH_3-TPD) temperature programmed reduction (TPR) of the catalysts have been performed to clarify the nature of the active and selective sites.

2. Experimental

2.1. Samples preparation

Au catalysts were prepared by deposition–precipitation in agreement with the Haruta's procedure [17]. The deposition–precipitation of gold onto the supports was carried out by adding the support to an aqueous solution of $HAuCl_4$ (Alpha Aesar assay ≥99.99%, Au 49.5%) previously adjusted at pH 7–8 with NaOH. The slurry was maintained at 343 K, under vigorous stirring, for 2 h. Then the samples were filtered, washed with deionized water until elimination of chloride then dried under vacuum at 353 K for one day.

Goethite (FeOOH), maghemite (γFe_2O_3) and hematite (αFe_2O_3) used as support are commercial products purchased by Aldrich. The gold content was determined by measuring the absorbance of gold solutions at $\lambda = 400$ nm [18]. The solutions were prepared dissolving the catalysts in $HCl–HNO_3$ (3:1 by volume), then adding a solution of tin(II) chloride in hydrochloric acid.

2.2. Samples characterization

Characterization was performed on solids previously soaked into ethanol and reduced in hydrogen flow, at 343 K for 1 h, with the aim to simulate the conditions of the working catalysts (see Section 2.3).

Specific surface area and porosity data were determined by adsorption–desorption of dinitrogen at 77 K, after outgassing (10^{-4} mbar) the sample at 353 K for 2 h using a Micromeritics ASAP 2010. Pore size distributions and pore volume were derived from the desorption isotherm at $P/P_0 \geq 0.3$.

XRD studies were carried out with an Ital-Structures diffractometer using nickel filtered Cu Kα radiation by mounting the powder samples on plexiglas holders. Diffraction peaks were compared with those reported in the JCPDS Data File.

TPR experiments were carried out in a conventional apparatus heating the sample (weight = 0.05 g) from room temperature to 800 K (heating rate 10 K/min) under 5% H_2/Ar (vol.%) with a constant flow rate of 20 cm^3/min. A molecular sieve cold trap (maintained at 193 K) and a tube filled with KOH were used to block water and CO_2, respectively, before the thermal conductivity detector (TCD).

The total acidity of the catalysts was measured by temperature programmed desorption of ammonia (NH_3-TPD). The NH_3-TPD instruments was equipped with a quadrupole mass spectrometer (Sensorlab VG Quadrupoles). The acidity was calculated from the amount of NH_3 adsorbed at room temperature and desorbed between 298 K and 773 K (heating rate 10 K/min). The quantification was made using pulse of known volume of NH_3.

HRTEM analysis were performed on a Philips instrument Model CM12 electron microscopy, operating at 200 kV and directly interfaced with a computer for real time image processing. The powdered samples were ultrasonically dispersed in isopropyl alcohol and then a few droplets of the above suspension deposited on a holey carbon support film copper grid. After evaporation of the solvent, the specimens were introduced into the microscope column. From each catalyst several hundred gold particles were measured in order to obtain a good statistical particle size distribution.

2.3. Catalytic activity

The catalytic experiments were carried out at atmospheric pressure under H_2 flow, at 333 K, in a 100 ml four-necked batch reactor fitted with a reflux condenser, dropping funnel, thermocouple and magnetic stirrer head coupled with a gas stirrer (Mod. MRK 1/20 - BR purchased by Premex Reactor).

The catalyst (weight 0.5–1g; particle size = 160–200 mesh) was added to 25 ml of solvent (ethanol) and treated at 343 K for 1 h under gaseous H_2.

The substrate (6×10^{-4} mol) was injected through one arm of the flask. The reaction mixture was stirred at 700 rpm.

The *trans*,4-phenyl,3-buten,2-one, (benzalacetone), (purity 99.8%) and *trans*,3-phenyl, propenal (cinnamaldehyde) (purity > 98%) were supplied by ACROS and Aldrich, respectively.

The progress of the reaction was followed by sampling a sufficient number of microsamples and analyzing them by means of GC–MS (Shimadzu GC-QP5000 Mod.).

The reaction products were separated on a CP-WAX Capillary column, (1.20 μm, 60 m, 0.32 mm).

Selectivities were calculated by the expression $S_i = C_i/\sum C_p$ where C_i is the concentration of product i and C_p is the total concentration of the products.

Preliminary tests carried out with different amounts of catalysts (0.2–1.0 g) grain size (80–200 mesh) and stirring rate (500–1000 rpm) indicated that under the conditions used the reaction is carried out in the absence of mass-transfer limitations.

3. Results and discussion

The chemical and morphological properties of gold catalysts are reported in Table 1. "AF" preparations have the same gold content whereas surface area varies within a wide range from 6 to 171 m^2/g. All the samples show a monomodal distribution of pore size and the mean pore diameter ranges between 4 and 11 nm.

The characterization of the commercial supports by X-ray diffraction shows that goethite is amorphous whereas maghemite and hematite are under crystalline form [8]. Upon addition of gold and reduction in H_2 at 343 K no structural changes of the supports have been evidenced and no additional peaks due to metallic gold are visible (Fig. 1).

In Table 1 are also reported the chemical and structural data of the Au/Fe_2O_3 reference catalyst, supplied by the World Gold Council. On this catalyst, prepared according with the coprecipitation method adopted by Haruta, the support is present as crystalline hematite, αFe_2O_3 (Fig. 1).

3.1. Particle size characteristics

For visual comparison of the four catalysts studied, low magnification views are given in Fig. 2a–d. From these figures it can be seen that the microstructure and the particles size of the supports are very different. Goethite (Fig. 2a) shows an homogeneous structure and aggregates of almost round and very small particles (around 3–5 nm in diameter). Maghemite (Fig. 2b) has an hexagonal close-packed morphology and a broad particles size distribution (10–100 nm). Commercial hematite (Fig. 2c) shows the well characteristic morphology of sintered powders likely due to the high temperature used during the preparation process whereas, on the Au/Fe_2O_3 reference catalyst hematite particles have a smaller diameter (Fig. 2d).

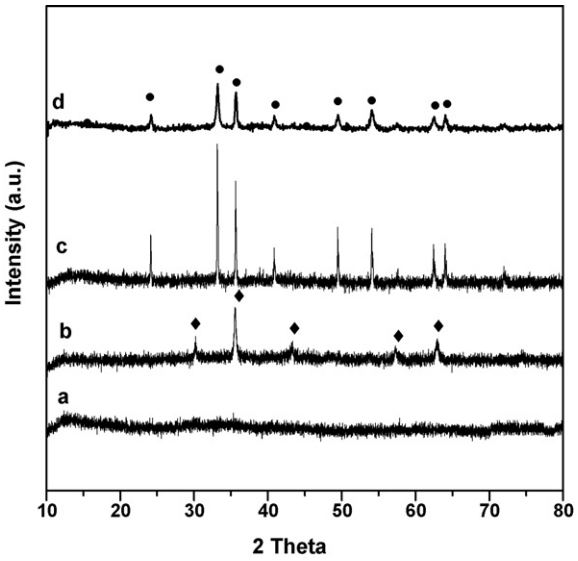

Fig. 1. XRD spectra of gold catalysts: (a) AF3.5G; (b) AF3.5M; (c) AF3.5H; (d) Au/Fe_2O_3 (◆) maghemite; (●) hematite.

With respect to the metal distribution from these figures it may be recognized that highly dispersed, nanometer-sized gold particles are present. All the samples show a monomodal distribution of gold particle size and the mean particle diameter, d_{Au}, together with the standard deviation (σ (nm)) are summarized in Table 1. Among the catalysts investigated, AF3.5H shows the broadest gold size distribution ($d_{Au} = 4.7 \pm 3.9$ nm).

A careful HRTEM analyses has been carried out in order to evaluate the shape of gold particles.

As already mentioned, the degree of rounding of gold particles is one of the critical parameters for the activity and selectivity to unsaturated alcohol in the gas-phase hydrogenation of acrolein [14].

Figs. 3–6 show representative gold particles of nearly the same size on different supports (αFe_2O_3, γFe_2O_3, FeOOH).

Table 1
Properties of gold catalysts

Catalyst	Au (wt.%)	Support	S.A. (m^2/g)	Average pore diameter (nm)	Mean gold particle size[a], d (nm)	Total acidity NH_3 TPD (μmolNH_3/m^2)
AF3.5G	3.5	FeOOH	171	4.0	4.3 ± 1.3	28.2
AF3.5M	3.5	γFe_2O_3	43	8.4	3.1 ± 1.5	6.6
AF3.5H	3.5	αFe_2O_3	6	6.8	4.7 ± 3.9	6.1
Au/Fe_2O_3[b]	4.4	αFe_2O_3	39	10.9	3.7 ± 1.5	8.6

[a] Measured by HRTEM.
[b] Gold reference catalyst, Type C, Lot no. Au/Fe_2O_3 #02-3.

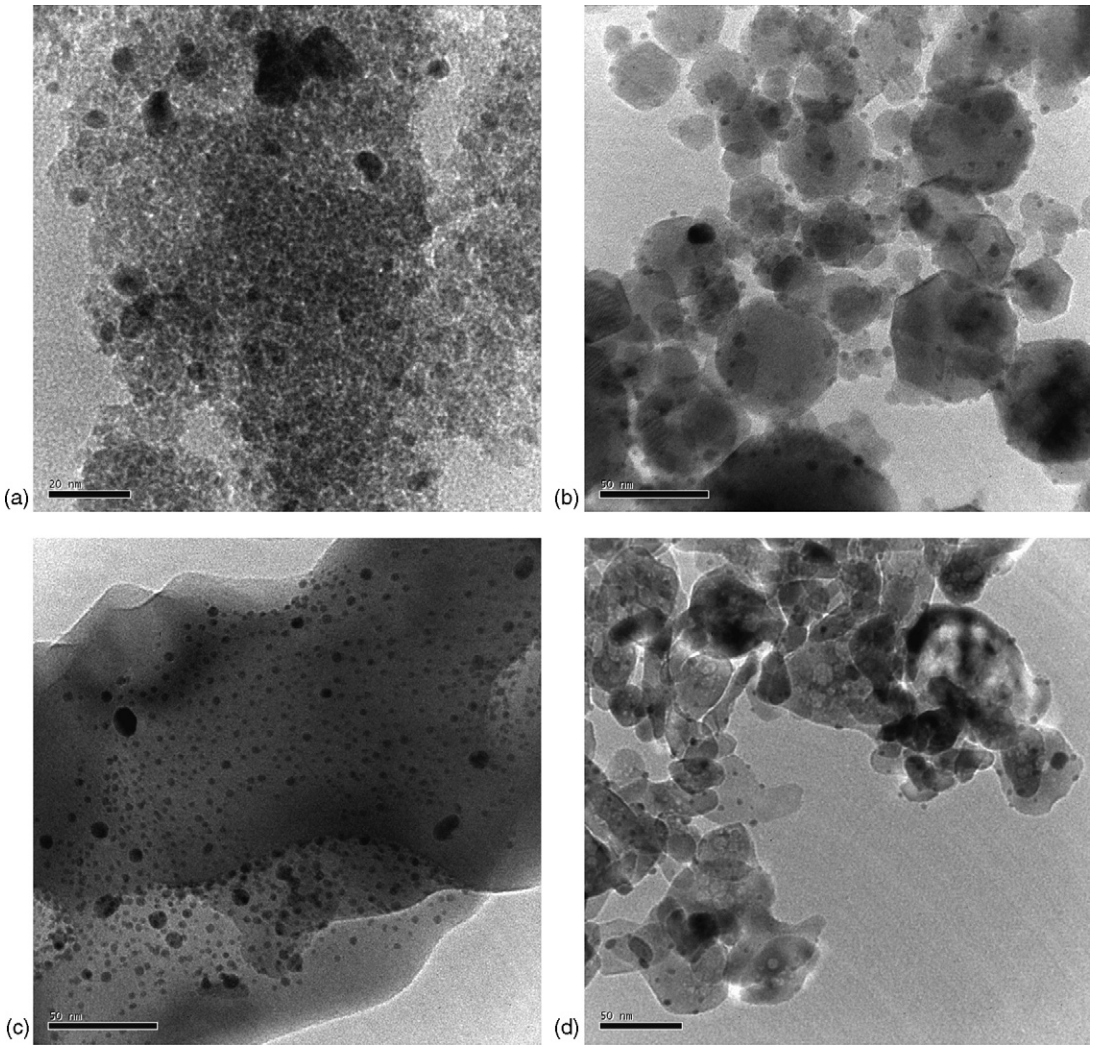

Fig. 2. HRTEM microphotographs of gold supported catalysts: (a) AF3.5G; (b) AF3.5M; (c) AF3.5H; (d) Au/Fe_2O_3.

HRTEM analyses in the cross sectional view show that Au particles dispersed on goethite have hemispherical (Fig. 3a) and nearly spherical shape (Fig. 3b).

Gold particles distributed on commercial hematite αFe_2O_3 and maghemite γFe_2O_3, AF3.5H and AF3.5M, respectively, mainly show an extended faceted surface (Figs. 4a and 5a). Metal particles attached to the support by their flat plane are also present (Figs. 4b and 5b).

On reference catalyst Au/Fe_2O_3, gold particles are mainly in hemispherical shape and they are attached to the support by their flat plane (Fig. 6a). Few gold particles show a faceted surface (Fig. 6b). Our observations are in good agreement with TEM results reported in 1993 by Haruta et al. [19] on Au/αFe_2O_3 catalyst prepared with the same procedure used for the preparation of reference catalyst.

From these results it is pointed out that within catalysts prepared by deposition precipitation the type of the support modifies the morphology of gold particles. Gold supported on amorphous goethite, AF3.5G, shows nearly spherical shape whereas on crystalline hematite and maghemite there is a predominance of faceted gold particle.

Moreover within hematite supported catalysts, on Au/Fe_2O_3 reference gold is mainly in hemispherical shape whereas on AF3.5H a faceted gold nanoparticles are obtained. It should be noted that on reference catalyst the support particles size are much lower than that of commercial hematite and that gold particles are mainly distributed on the outer shell of the grains. On commercial hematite, instead, gold particles are distributed on the flat surface of the support which in turn can determine a change in the morphology of the metal particles.

3.2. Surface acidity measurements

The total acidity of the catalysts was measured by temperature programmed desorption of NH_3 (NH_3-TPD) adsorbed at room temperature. In Fig. 7 are reported the desorption profiles of all the samples investigated. On gold supported on goethite and hematite (Fig. 7a, c and d) a broad peak of NH_3 desorption, with a T_{max} centered at 630 K is observed. In addition, gold catalysts supported on hematite (Fig. 7c and d) show a broad and less intense desorption peak of NH_3 at lower temperature. Au supported on maghemite

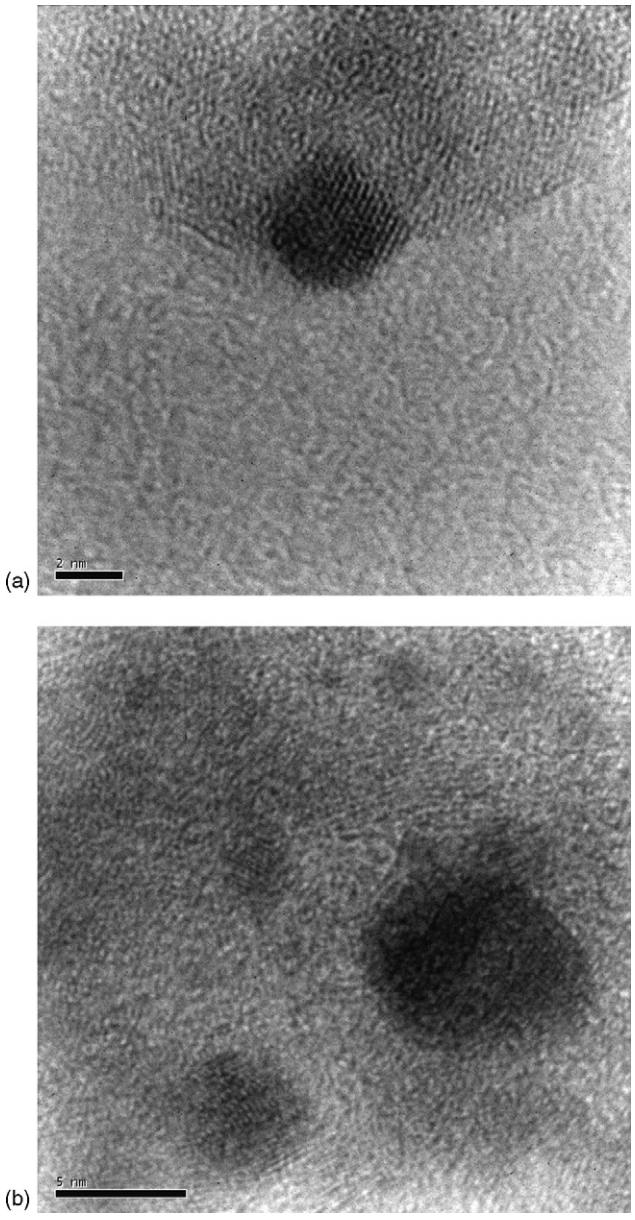

Fig. 3. Representative gold particles of sample AF3.5G.

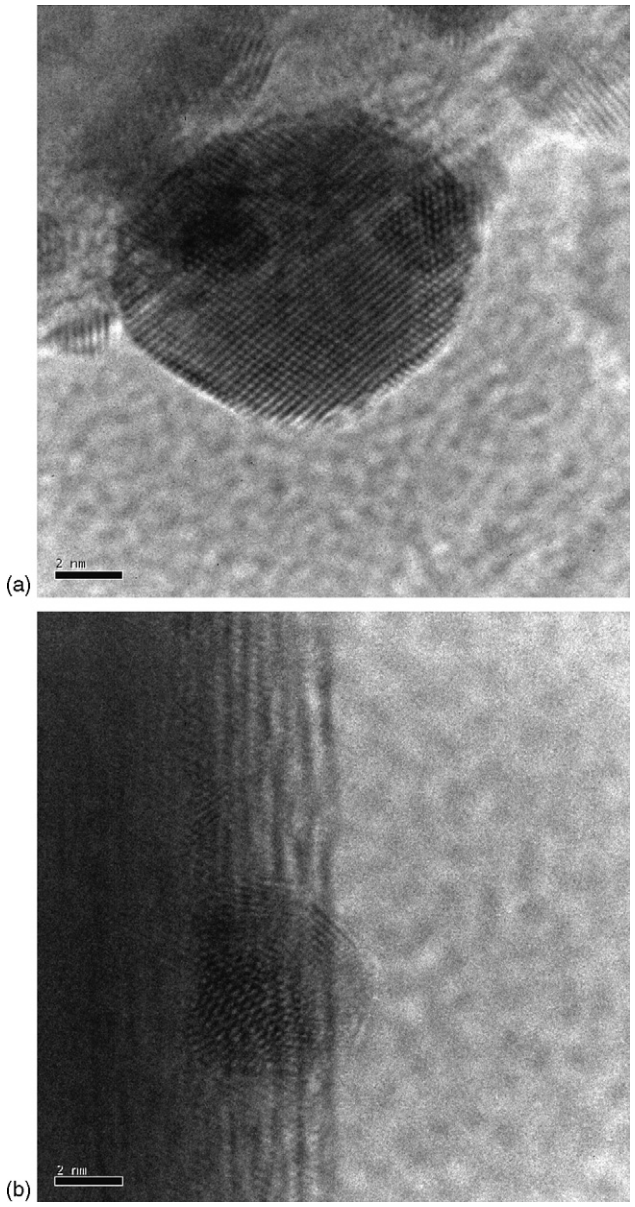

Fig. 4. Representative gold particles of sample AF3.5H.

(Fig. 7b), instead, shows only a very broad desorption peak in the temperature range 370–550 K.

From a qualitative analysis it can be observed that Au supported on goethite and hematite have stronger acid sites than Au supported on maghemite.

The total acidity, expressed as μmol of NH_3 desorbed/m^2 is reported in Table 1. It can be seen that Au supported on hematite and maghemite show a similar density of acid sites. An abrupt increase of the total acidity is observed on Au supported on goethite.

3.3. TPR measurements

The reducibility of catalysts and of the parent supports have been investigated by means of temperature programmed reduction (TPR). The reduction profiles of the supports show one peak of reduction (Fig. 8a–c) in the range of temperature investigated. The amount of hydrogen consumed, H, calculated from the area under the peak corresponds to the reduction of Fe(III) to magnetite, Fe_3O_4. This is outlined from the ratio H/H_t (Fig. 8) where H_t represents the theoretical amount of hydrogen which is necessary for the reduction step of Fe(III) to Fe_3O_4.

Goethite, FeOOH (Fig. 8a) and maghemite, γFe_2O_3 (Fig. 8b) are reduced at lower temperature with respect to hematite, αFe_2O_3.

Upon addition of gold the reducibility of catalysts enhance (Fig. 9a–c). On all the catalysts investigated the ratio H/H_t, is close to 1 (Fig. 9) thus indicating that gold is under metallic state.

On gold supported on goethite and maghemite (Fig. 9a and b) the reduction peak is shifted by ≈200 K at lower temperature with respect to that of the supports whereas on gold supported on hematite (Fig. 9d) the temperature shift is less pronounced

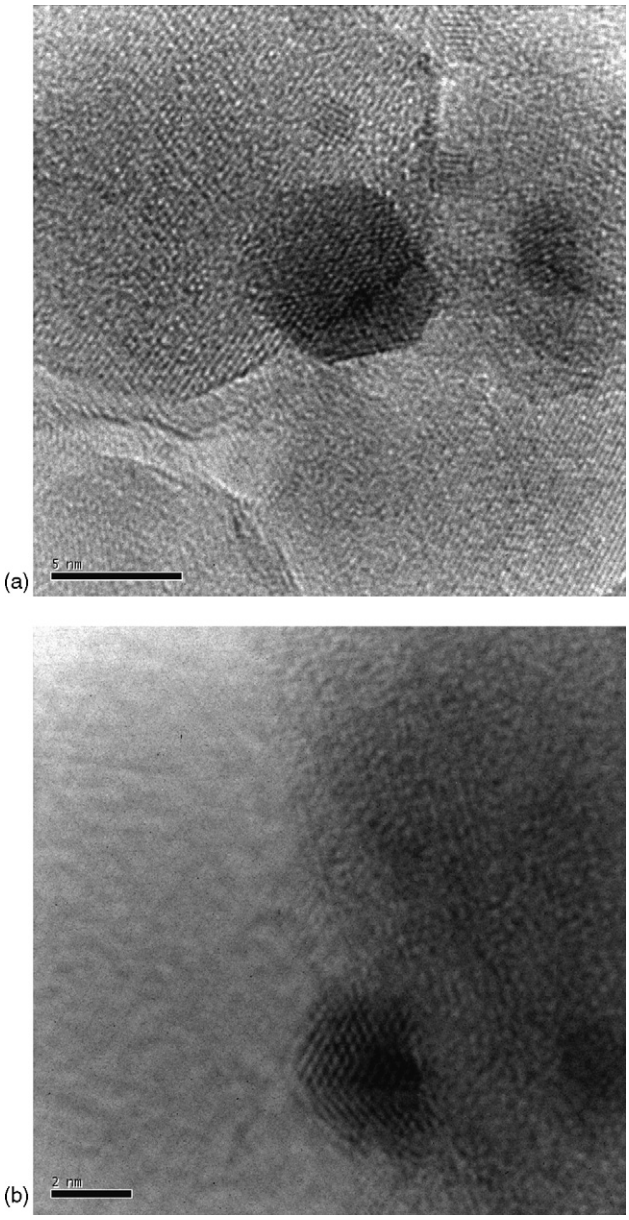

Fig. 5. Representative gold particles of sample AF3.5M.

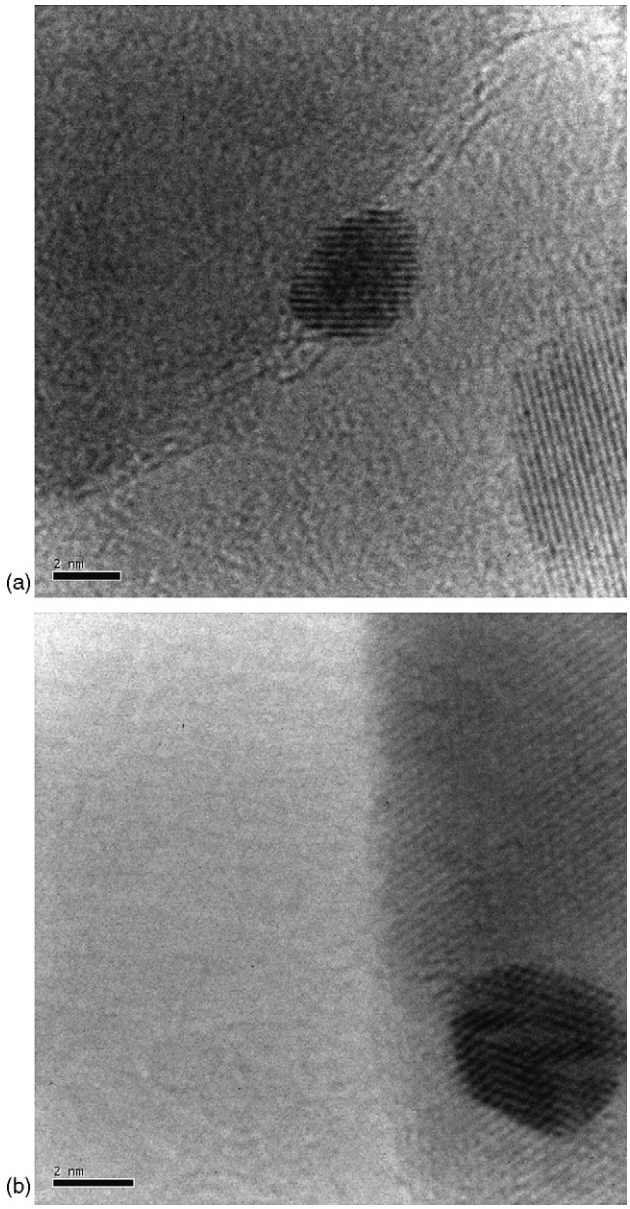

Fig. 6. Representative gold particles of sample Au/Fe_2O_3.

(≈90 K). As matter of comparison is also reported the TPR profile of the reference catalyst (Fig. 9c). It can be seen that the reduction temperature is lower than that observed on the AF3.5H likely due to its higher surface area. The influence of the surface area on the reduction temperature of Fe_2O_3 to magnetite has been pointed out by Neri et al. [20]. The authors have reported that on similar iron oxide phase the increase of the surface area causes a shift of the reduction temperature to lower values [20].

3.4. Catalytic activity in the hydrogenation of benzalacetone and cinnamaldehyde

On all the gold preparations the hydrogenation of α,β unsaturated carbonyl compounds follows a reaction pathways reported in Scheme 1.

The hydrogenation of the conjugated C=C bond and C=O bond occurs through two parallel reactions. At high conversion of the substrate (>80%) the saturated carbonyl compound is further hydrogenated to the corresponding saturated alcohol. The hydrogenation of the unsaturated alcohol hardly occurs even at quantitative conversion of unsaturated ketone or aldehyde.

In the hydrogenation of cinnamaldehyde the formation of acetals of cinnamaldehyde and hydrocinnamaldehyde were also observed. As reported by several authors the formation of acetals from aldehyde and ethanol used as solvent, is catalysed by acid sites [21–24]. Acetals are always in equilibrium with the respective aldehydes [22–24] therefore, for simplification, cinnamaldehyde and hydrocinnamaldehyde are reported together with their respective acetals.

The hydrogenation of benzalacetone and cinnamaldehyde follows a pseudo-first-order reaction rate law with respect to the

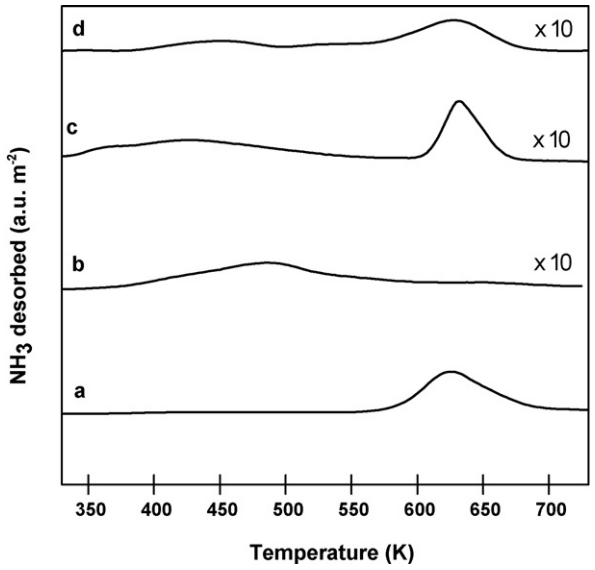

Fig. 7. NH_3-TPD desorption profiles of gold supported catalysts: (a) AF3.5G; (b) AF3.5M; (c) Au/Fe_2O_3; (d) AF3.5H.

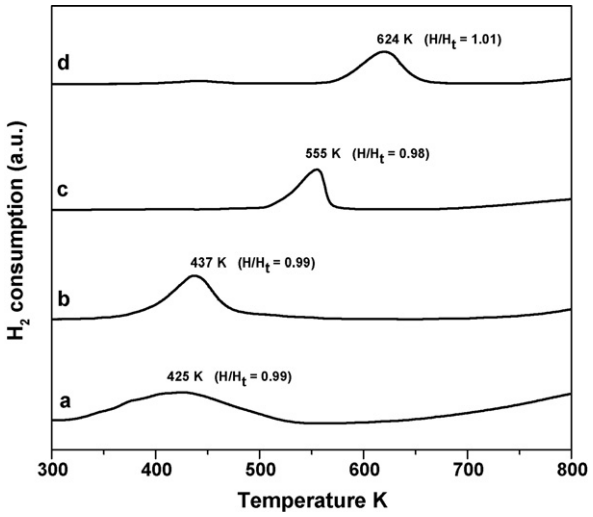

Fig. 9. TPR of gold catalysts: (a) AF3.5G; (b) AF3.5M; (c) Au/Fe_2O_3; (d) AF3.5H. In bracket is reported the ratio H/H_t where H is the hydrogen consumed and H_t is the theoretical hydrogen for the reduction of Fe(III) to magnetite (Fe_3O_4).

organic substrate. The first-order rate constant $K_{aldehyde}$ and K_{ketone} (min^{-1} $g_{cat}{}^{-1}$) are reported in Table 2. It can be seen that in the hydrogenation of benzalacetone and cinnamaldehyde the catalytic activity ranks in the order AF3.5G > AF3.5M > AF3.5H > Au/Fe_2O_3. The lower activity measured in the hydrogenation of cinnamaldehyde with respect to that of benzalacetone can be explained considering that due to the partial transformation of cinnamaldehyde to acetals the concentration of aldehyde available for hydrogenation is lower with respect to the concentration of benzalacetone.

The catalytic activity of gold catalysts cannot be simply related with the mean gold particle size. All the catalysts investigated, indeed, show a very close mean particle size (Table 1) but different activity. Claus et al. [14] have reported

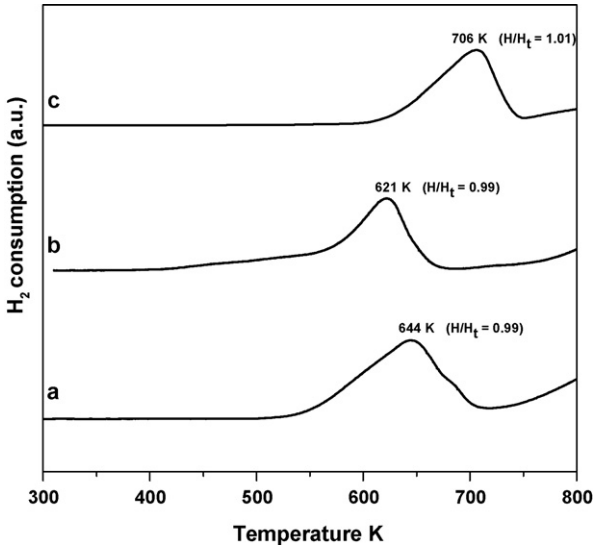

Fig. 8. TPR profiles of iron oxide supports: (a) FeOOH; (b) γFe_2O_3; (c) αFe_2O_3. In bracket is reported the ratio H/H_t where H is the hydrogen consumed and H_t is the theoretical hydrogen for the reduction of Fe(III) to magnetite (Fe_3O_4).

that the particle size dependence of activity and selectivity of gold catalysts in the hydrogenation of acrolein is a cooperative effect of particle size and the degree of rounding of gold particles and the highest catalytic activity was found on catalysts having a larger portion of metal particles with a spherical shape, i.e. high degree of rounding. HRTEM analyses have shown that within gold supported on hematite, Au/Fe_2O_3 reference has gold particles with hemispherical shape (Fig. 6a) whereas on AF3.5H gold particles are clearly well facetted (Fig. 4). Despite the higher degree of rounding of metal particles in the reference catalyst its catalytic activity is lower than activity of AF3.5H. For sake of clarity it should be also considered that the lower activity of reference can also arise from the different pre-treatment of the sample. Au/Fe_2O_3 reference has been calcined at 773 K whereas our catalysts have been reduced under very mild conditions (343 K). Previously it has been found that calcination of the solid is detrimental for the catalytic activity in the hydrogenation of benzalacetone [7]. A further evidence of the negligible role of the shape of gold particles on the activity arises from the comparison of the activity of AF3.5M and AF3.5H. Despite the similar metal particles shape (Figs. 4 and 5) the catalytic activity is strongly different and AF3.5M is more active than AF3.5H (Table 2).

These results suggest that in the hydrogenation of benzalacetone and cinnammaldehyde the morphology of gold particles has a scarce influence on the catalytic activity which seems mainly influenced by the nature of the support. On the most active AF3.5G catalysts nearly spherical gold particles are present (Fig. 3) but, at light of previous results, it is likely that the highest activity is mainly generated from the different nature of the support.

It seems that the surface area of catalysts has less influence on the catalytic activity. Indeed, catalysts with similar surface area, Au/Fe_2O_3 reference and AF3.5M, show large differences in the catalytic activity (Table 2).

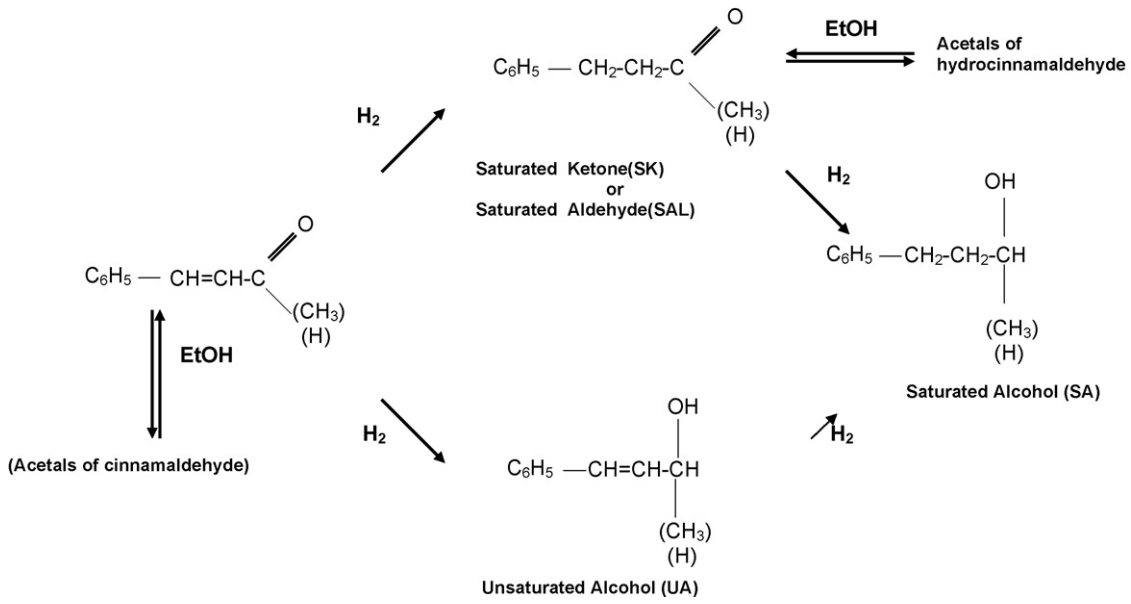

Scheme 1. Reaction network of the hydrogenation of unsaturated carbonyl compounds.

There are a lot of evidence that together with the size and the shape of the Au particles the hetero-junction between the Au particles and a metal oxide support seems to be the key element for generating the catalytic activity of Au catalysts [25–28]. The nature of the support can deeply influence the electronic state of gold than its catalytic properties. XPS experiments have shown the existence of positively charged Au atoms on Au/CeO_2 catalyst [29]. The formation of negatively charged gold particles was observed upon reduction in H_2 of Au supported on TiO_2 and ZrO_2 catalysts at 773 K and 573 K, respectively [2,16–30]. The increase of the electronic density of the metal upon reduction has been explained claiming an electron transfer from the partial reduced support to the metal [30].

Negatively charged Au nanoparticle has a stable chemisorption state of H atom and has an ability to dissociate H_2 at low temperature [31].

In our case, it can be argued that due to the pre-treatment ''in situ'' of the catalysts with hydrogen, before the reaction, a partial reduction of the support occurs. Under these conditions negatively charged Au nanoparticles could be formed through an electron transfer from the reduced support to the anchored gold metal [16–30]. Due to the low temperature (343 K) at which the pre-reduction of the catalysts is carried out it is likely that the degree of reduction of the support increases with the reducibility of the catalysts. As a result the electron density on gold nanoparticles and/or the number of negatively charged gold particles should also increase with the reducibility of the catalyst.

Therefore we have correlated the catalytic activity of catalysts with their reducibility, in terms of T_{max} of reduction. In Fig. 10 are reported the rate constant calculated in the hydrogenation of benzalacetone and cinnamaldehyde versus the T_{max} of reduction of Au catalysts (Fig. 9) and it is shown that the catalytic activity increases with the reducibility of catalysts.

The existence of this correlation, even if it is not a direct proof, however suggests that negatively charged gold nanoparticles could be the active sites for hydrogenation reactions and that the reducibility of the supports strongly contributes to the formation of these sites. The increase of the catalytic activity on the most reducible catalysts could be due to the

Table 2
First-order rate constant measured in the hydrogenation of benzalacetone (K_{ketone}) and cinnamaldehyde ($K_{aldehyde}$) on gold catalysts

Catalyst	Au (wt.%)	K_{ketone} (min^{-1} g_{cat}^{-1}) 10^3	$K_{aldehyde}$ (min^{-1} g_{cat}^{-1}) 10^3
AF3.5G	3.5	9.0	5.7
AF3.5M	3.5	6.6	3.4
AF3.5H	3.5	1.8	0.6
Au/Fe_2O_3[a]	4.4	0.6	0.4

[a] Gold reference catalyst, Type C, Lot no. Au/Fe_2O_3 #02-3.

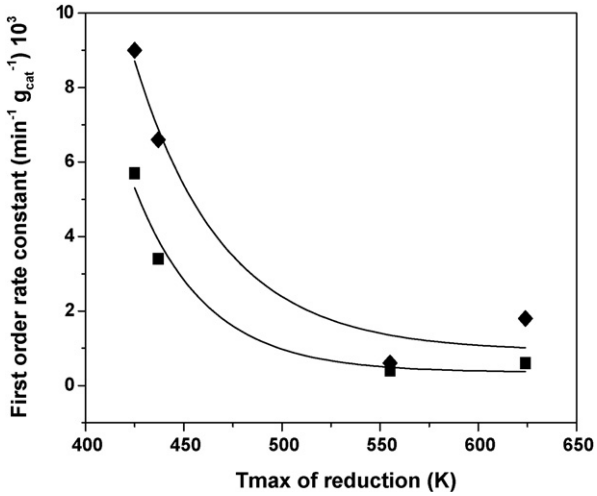

Fig. 10. Correlation between the first-order rate constant and T_{max} of reduction of gold catalysts. (◆) K_{ketone} (min^{-1} g_{cat}^{-1}), and (■) $K_{aldehyde}$ (min^{-1} g_{cat}^{-1}).

Table 3
Selectivity towards reaction products, measured at 50% of conversion, in the hydrogenation of cinnamaldehyde and benzalacetone on gold catalysts

Catalyst	Au (wt.%)	Products distribution in the hydrogenation of cinnamaldehyde			Products distribution in the hydrogenation of benzalacetone		
		Sel (%), SAL	Sel (%), UA	Sel (%), SA	Sel (%), SK	Sel (%), UA	Sel (%), SA
AF3.5G	3.5	6	91	3	14	64	21
AF3.5M	3.5	13	86	1	31	56	13
AF3.5H	3.5	54	44	2	94	6	2
Au/Fe_2O_3[a]	4.4	21	77	2	77	20	3

SAL: saturated aldehyde; UA: unsaturated alcohol; SA: saturated alcohol; SK: saturated ketone.
[a] Gold reference catalyst, Type C, Lot no. Au/Fe_2O_3 #02-3.

higher ability of negatively charged gold nanoparticles to dissociate hydrogen [31]. Moreover, accordingly with Claus et al. [2], negatively charged Au particles larger than 2 nm could also promote the activation of the organic substrate and in particular the activation of the conjugated C=O bond over that of C=C bond. It should be also considered that the activation of the substrate could be enhanced through a direct electron transfer from the reduced support to the reactant [30].

3.5. Products distribution in the hydrogenation of cinnamaldehyde

In Table 3 is reported the products distribution in the hydrogenation of cinnamaldehyde at conversion $\geq$50%, for all the catalysts investigated. The highest selectivity towards the formation of UA has been obtained on Au supported on goethite, AF3.5G, and maghemite, AF3.5M. Au/Fe_2O_3 reference shows an intermediate value of selectivity whereas AF3.5H shows the lowest selectivity to UA.

The selectivity towards the formation of UA cannot be correlated with the morphological properties of gold. Catalysts having similar metal particle size, AF3.5G and AF3.5H, (Table 1) show a different selectivity towards the formation of UA. On AF3.5G the selectivity is 91% whereas on AF3.5H it decreases up to 44%. Moreover it seems that the shape of gold particles has a scarse influence in the products distribution. On one hand, within gold catalysts supported on hematite, we have observed that the selectivity towards the hydrogenation of C=O is higher on Au/Fe_2O_3 catalyst, where gold particles have mainly hemispherical shape (Fig. 6a), with respect to AF3.5H having faceted gold particles (Fig. 4). But, comparing catalysts having similar shape, AF3.5M and AF3.5H (Figs. 4 and 5) it can be seen that the selectivity to UA on gold supported on maghemite (AF3.5M) is higher than that obtained on gold supported on hematite (AF3.5H).

Therefore, as already observed for the catalytic activity, also the selectivity towards the formation of UA in the hydrogenation of cinnamaldehyde strongly depends on the nature of the support and the modification of the shape of gold particles plays a minor role.

The influence of the support in the selective hydrogenation of α,β unsaturated aldehydes was widely investigated [32] and beside the change on the morphology of metal particles other effects have been considered such as: (i) steric effect on the molecule adsorption; (ii) promotion of the conjugated C=O bond; (iii) electronic effect on the metal.

The steric effect of the support deals with the spatial constraints, specially present in microporous materials, which orientate adsorption of the reactant molecules [32]. Blackmond et al. [33] have found that in the hydrogenation of cinnamaldehyde on transition metals supported on activated carbon and NaY, KY zeolites, the highest selectivity has been achieved on metal zeolite catalysts due to the molecular constraints of the reactant in the zeolite micropores ($d < 2$ nm). In these conditions the adsorption of the end C=O group is favourite whereas the adsorption of the C=C is dramatically hampered.

The support can promote the hydrogenation of the conjugated C=O through its adsorption via the lone pair of the oxygen atom on the electrophilic or Lewis acid sites at the interface with metal particle or migrating from oxide support to the metal surface upon high temperature reduction (SMSI effect) [9,32].

The electronic effect of the support on the metal is explained claiming an enrichment of the metal surface with electrons by interaction with a support which in turn enhances the hydrogenation rate of the C=O bond over that of the C=C bond due to the backbonding interaction with π^*C=O to a larger extent than with π^*C=C [32].

In our case several reasons suggest that the steric effect of the support on the selectivity to UA can be ruled out. First of all catalysts are mainly mesoporous (Table 1) with dimension of pore large enough to allow a good mobility of the substrate. Moreover, it has been observed that upon dispersion of gold on commercial hematite and maghemite a negligible decrease of the pore volume occurs thus indicating that the metal is mainly distributed on the external surface of the supports. These catalysts show strong differences in selectivity to UA (Table 3).

With respect to the role of the support as promoter in the activation of the C=O bond through coordination at acid sites a direct correlation between the total amount of acid sites or the strength of acid sites and selectivity to UA cannot be drawn suggesting that this effect is negligible in the hydrogenation of cinnamaldehyde on Au supported on iron oxides catalysts.

NH_3-TPD data (Table 1) show that on Au/Fe_2O_3 AF3.5H, AF3.5M, the density of acid sites is almost similar but they show very different selectivity to UA (Table 3). With respect to the strength of acid sites it has been found that AF3.5G shows stronger acid sites than AF3.5M (Fig. 7a and b) but the

selectivity to UA of AF3.5M is slightly lower than that of AF3.5G.

It is also reported that metallic iron acts as a promoter in the selective hydrogenation of α,β unsaturated aldehydes to unsaturated alcohols on Pt catalysts [32]. The mechanism of promotion by metallic iron has been explained considering an electron transfer from the more electropositive Fe to Pt and the electron deficient iron atoms act as Lewis adsorption sites for the C=O bond [32]. Electron transfer from iron to platinum can also increase the hydridic character of chemisorbed hydrogen and thus the nucleophilic attack by H^- species on the positively charged carbon of the polarized C=O bond [32]. In our case due to the mild conditions used to reduce the catalysts (T = 343 K) it can be ruled out that iron oxide are reduced, even partially, to metallic iron. This conclusion is supported by TPR experiments where it is shown that the presence of gold mainly promotes the partial reduction of Fe(III) oxide to magnetite (Fe_3O_4) whereas the further reduction to metallic iron occurs at temperature higher than 800 K [20].

A good correlation has been found between the selectivity towards the formation of UA and the reducibility, in terms of T_{max} of reduction, of the catalysts. In Fig. 11, it is shown that the selectivity to UA increases when the T_{max} of reduction decreases. Our hypothesis is that the support influences the electronic state of gold nanoparticles than their catalytic properties through an electron transfer from the reduced support to the metal. The higher charge density on metal surface atoms favors the backbonding interaction with the π^*C=O orbital to a larger extent than with π^*C=C orbital, so that the hydrogenation of the C=O group should be favored over that of the C=C group.

3.6. Products distribution in the hydrogenation of benzalacetone

In Table 3 is also reported the products distribution in the hydrogenation of the benzalacetone at conversion ≥50%, for all the catalysts investigated.

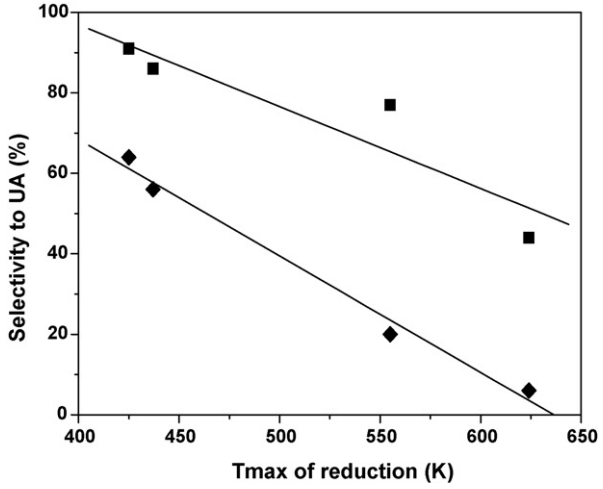

Fig. 11. Correlation between the selectivity towards the unsaturated alcohol, measured at conversion ≥50%, and T_{max} of reduction of gold catalysts. (◆) UA from hydrogenation of benzalacetone; (■) UA from hydrogenation of cinnamaldehyde.

It can be seen that the selectivity towards the formation of the unsaturated alcohol ranks in the order AG3.5G > AF3.5M > Au/Fe_2O_3 > AF3.5H, as already observed in the hydrogenation of cinnamaldehyde. It should be noted that the selectivity towards UA in the hydrogenation of the unsaturated ketone is always lower than that obtained in the hydrogenation of cinnamaldehyde. This can be due to a higher steric hindrance of C=O in the ketone. Due to the similar behavior of gold catalysts towards the hydrogenation of the C=O bond in the hydrogenation of benzalacetone and cinnamaldehyde and at light of the previous discussion it can be concluded that also in the hydrogenation of benzalacetone the selectivity towards the formation of UA is strongly influenced by the support and, as shown in Fig. 11, increases with the reducibility of the catalysts.

The main role of the support seems to be the formation of electron enriched gold particles through an electron transfer from the reduced support to the metal On these sites the backbonding interaction with the π^*C=O orbital is favoured, so that the hydrogenation of the C=O group increases over that of the C=C group.

From these results it can be also concluded that the hydrogenation of α,β unsaturated ketone and aldehyde on gold supported on iron oxides catalysts occurs with the same mechanism.

4. Conclusions

The results reported in this paper show that the catalytic activity and selectivity to UA in the hydrogenation of benzalacetone and cinnamaldehyde on gold supported on iron oxides catalysts are scarcely influenced by the shape of gold particles whereas are strongly influenced by the nature of the support.

A good correlation has been found between the reducibility of the catalysts and the catalytic activity and selectivity towards the hydrogenation of the conjugated C=O.

Increasing the reducibility of the catalysts the catalytic activity and selectivity increases. These results let us to argue that active and selective sites are formed by negative gold particles formed through the electron transfer from the reduced support to the metal. The increase of the catalytic activity with the reducibility of the catalysts could be due to an increase of the electron density on gold nanoparticles and/or to an increase of the number of negatively charged gold particles on which dissociation of hydrogen occurs at low temperature. It should be also considered that the increase of the catalytic activity can be due to an enhancement of the activation of the organic substrate on negatively charged metal particles and/or through a direct electron transfer from the reduced support to the reactant. The increase of the selectivity towards the formation of UA with the reducibility of the catalysts has been explained considering that on a more electron enriched gold particles the backbonding with the π^*C=O orbital is favoured, so that the hydrogenation of the C=O group increases over that of the C=C group.

References

[1] C. Mohr, H. Hoefmeister, M. Lucas, P. Claus, Chem. Eng. Technol. 3 (2000) 324.
[2] P. Claus, A. Brückner, C. Mohr, H. Hofmeister, J. Am. Chem. Soc. 122 (2000) 11430.
[3] J.E. Bailie, H.A. Abdullah, J.A. Anderson, C.H. Rochester, N.V. Richardson, N. Hodge, J.G. Zhang, A. Burrows, C.J. Kiely, G.J. Hutching, Phys. Chem. Chem. Phys. 3 (2001) 4113.
[4] C. Milone, M.L. Tropeano, G. Gulino, G. Neri, R. Ingoglia, S. Galvagno, J. Chem. Soc., Chem. Commun. (2002) 868.
[5] R. Zanella, C. Louis, S. Giorgio, R. Touroude, J. Catal. 223 (2004) 328.
[6] C. Milone, R. Ingoglia, M.L. Tropeano, G. Neri, S. Galvagno, J. Chem. Soc., Chem. Commun. (2003) 868.
[7] C. Milone, R. Ingoglia, A. Pistone, G. Neri, F. Frusteri, S. Galvagno, J. Catal. 222 (2004) 348.
[8] C. Milone, R. Ingoglia, L. Schipilliti, C. Crisafulli, G. Neri, S. Galvagno, J. Catal. 236 (2005) 80.
[9] V. Ponec, Appl. Catal. A: Gen. 149 (1997) 27.
[10] R.L. Augustine, Catal. Today 37 (1997) 419.
[11] J. Kaspar, M. Graziani, G. Picasso Escobar, A. Trovarelli, J. Mol. Catal. 72 (1992) 243.
[12] M. Gargano, V. D'Orazio, N. Ravasio, M. Rossi, J. Mol. Catal. 58 (1990) L5.
[13] S.N. Coman, V.I. Parvulescu, M. De Bruyn, D.E. De Vos, P. Jacobs, J. Catal. 206 (2002) 218.
[14] C. Mohr, H. Hofmeister, P. Claus, J. Catal. 213 (2003) 86.
[15] C. Mohr, H. Hofmeister, J. Radnik, P. Claus, J. Am. Chem. Soc. 125 (2003) 1905.
[16] J. Radnik, C. Mohr, P. Claus, Phys. Chem. Chem. Phys. 5 (2003) 172.
[17] M. Haruta, Catal. Tech. 63 (2002) 102.
[18] F.E. Beamish, J.C. van Loon, Analysis of Noble Metals, Academic Press, New York, 1977.
[19] M. Haruta, S. Tsubota, T. Kobayashi, H. Kageyama, M.J. Genet, B. Delmon, J. Catal. 144 (1993) 175.
[20] G. Neri, A.M. Visco, S. Galvagno, M. Panzalorto, Thermochim. Acta 329 (1999) 39.
[21] M. Lashdaf, V.-V. Nieminen, M. Tiita, T. Vanalainen, H. Osterholm, O. Krouse, Micropor. Mesopor. Mater. 75 (2004) 149.
[22] S. Galvagno, G. Capannelli, G. Neri, A. Donato, R. Pietropaolo, J. Mol. Catal. 64 (1991) 237.
[23] B. Coq, P.S. Kumbar, C. Moreau, P. Moreau, M.G. Warawdekar, J. Mol. Catal. 85 (1993) 215.
[24] L. Zhang, M. John, A.P. Winterbottom, S. Boyes, Raymahasay, J. Chem. Tech. Biotechnol. 72 (1998) 264.
[25] S. Tsubota, D.A.H. Cunningham, Y. Bando, M. Haruta, in: B. Delmon (Ed.), Preparation of Catalysts VI, Elsevier, Amsterdam, 1995, p. 227.
[26] S. Tsubota, F. Boccuzzi, Y. Iizuka, M. Haruta, Shokubai, J. Catal. 38 (1996) 422.
[27] M. Haruta, Catal. Today 36 (1997) 153.
[28] M. Haruta, Chem. Rec. 3 (2003) 75.
[29] Q. Fu, H. Saltsburg, M. Flytzani-Stephanopoulos, Science 301 (2003) 935.
[30] S. Schimpf, M. Lucas, C. Mohr, U. Rodemerck, A. Bruckner, J. Radnik, H. Hofmeister, P. Claus, Catal. Today 72 (2002) 63.
[31] M. Okumura, Y. Kitagawa, M. Haruta, K. Yamaguchi, Appl. Catal. A: Gen. 291 (2005) 37.
[32] P. Gallezot, D. Richard, Gallezot, Catal. Rev. Sci. Eng. 40 (1998) 81.
[33] D.J. Blackmond, R. Oukaci, B. Blanc, P. Gallezot, J. Catal. 131 (1991) 411.